Journal of Materials Chemistry B

PAPER

View Article Online
View Journal | View Issue

Cite this: J. Mater. Chem. B, 2015, 3, 458

A simple strategy based on upconversion nanoparticles for a fluorescent resonant energy transfer biosensor†

Hao Zhu,[a] Yujie Ding,[ab] Anqi Wang,[a] Xu Sun,[a] Xing-Cai Wu*[a] and Jun-Jie Zhu*[a]

Received 9th August 2014
Accepted 15th October 2014

DOI: 10.1039/c4tb01320d

www.rsc.org/MaterialsB

A novel aptasensor was fabricated for the detection of lysozyme and DNA based on the fluorescence resonance energy transfer (FRET) technique between upconversion nanoparticles (UCNPs) and a dye labeled aptamer. UCNPs can act as excellent emitters due to their low autofluorescence and high penetration depth of biosamples. $NaYF_4$:Yb, Er nanoparticles as UCNPs were synthesized and attached with a dye labeled aptamer through a cationic polymer as an electrostatic linker to quench the upconversion fluorescence intensity. The intensity can be restored after the addition of lysozyme or the complementary DNA (target DNA) because of their strong interaction with the aptamer. The sensor provided a linear concentration range from 30 to 210 nM for lysozyme and 40 to 200 nM for the target DNA, the limit of detection was 2.5 nM and 2.8 nM, respectively. The sensor was also used to monitor the lysozyme level in both human saliva and serum samples, and the results were consistent with the reported values. The method was simple and convenient without the extra procedure of bioconjugation, and could be put to use for the determination of various targets in the future.

1. Introduction

In recent years, rare earth luminescent materials have shown wide use in optical fiber telecommunications, light-emitting organic electroluminescence applications, lighting and other areas of biomedicine. Among those materials, upconversion nanoparticles (UCNPs) attract the most focus due to their unique optical and chemical properties, such as sharp absorption and emission bands, high quantum yields, long lifetimes and superior photostability.[1–3] UCNPs are usually composed of oxides, fluorides, halogen oxides or other substrates as the matrix and doped with trivalent rare earth ions (Er^{3+}, Eu^{3+}, Yb^{3+}, Tm^{3+}, Ho^{3+} *etc.*) as the energy transfer system. UCNPs can convert low-energy light (NIR or IR) to higher-energy light (UV or visible) through multiple photon absorptions or energy transfers; as a result, the UCNPs exhibit low autofluorescence from biosamples and better penetration depth than the traditional downconversion fluorescent materials.[4–8] Therefore, UCNPs can be used as suitable candidates in sensing and bioimaging.

Aptamers obtained with systematic evolution of ligands by exponential enrichment (known as SELEX) are usually single-stranded DNA or RNA oligonucleotides.[9] Aptamers can bind specifically to various target molecules, including amino acids, antibiotics, peptides, vitamins, proteins and even whole cells.[10] In general, aptamers can be viewed as an ideal replacement for antibodies because of their small size, simple preparation, good stability, high reproducibility and easy modification.[11] Nowadays, a large number of analytical approaches are being used to fabricate aptamer-based sensors for protein detection, among which the fluorescence resonance energy transfer (FRET) process is often adopted.[12–16] For a well-designed FRET system, the donor and acceptor can be brought to a proper distance from each other exclusively through the recognition of target substances, leading to a corresponding change in fluorescence intensity. Since Wang reported a FRET biosensor using UCNPs in 2005,[17] UCNPs have been selected as energy donors in the FRET system. Besides gold nanoparticles, fluorescent dyes and carbon materials have been used as energy acceptors.[18–24] Although inorganic materials are able to quench donors with high efficiency, they also bring about instability in the system. In addition, the UCNPs in the systems are often converted to the related oligonucleotides using cross-linkers (EDC or DDC), which needs several complicated steps and may decrease the efficiency.[3,25] To simplify the assembly, it is desirable to find a novel strategy without the extra procedure of bioconjugation.

[a]State Key Laboratory of Analytical Chemistry for Life Science, School of Chemistry and Chemical Engineering, Nanjing University, Nanjing, 210093, P. R. China. E-mail: wuxingca@nju.edu.cn; jjzhu@nju.edu.cn; Fax: +86-25-83597204; Tel: +86-25-83597204

[b]College of Biochemical Engineering, Anhui Polytechnic University, Wuhu, 241000, P. R. China

† Electronic supplementary information (ESI) available. See DOI: 10.1039/c4tb01320d

Lysozyme is a ubiquitous protein serving as a natural drug by cleaving acetyl groups in the polysaccharide walls of bacteria and exists universally in body tissues and secretions.[26] The enzyme has a molecular weight of about 14.3 kDa and an isoelectric point value (pI) of 11.0. The abnormal levels of this kind of enzyme in saliva, serum and urine have been associated with many diseases, such as leukemia, meningitis, HIV and renal diseases.[27] Although some strategies have been reported for lysozyme detection,[26,28–32] only very few have been reported for detection using UCNPs *via* the FRET technique.

Herein, we report a simple sensing platform for lysozyme and the complementary DNA (target DNA) determination based on FRET between fluorescent UCNPs and a dye-labeled aptamer through a cationic polymer as an electrostatic linker, which can avoid the complicated covalent immobilization and modification of UCNPs.

2. Experimental section

2.1 Materials

All starting materials were obtained from commercial suppliers and used as received. $YCl_3 \cdot 6H_2O$ (99.99%), $YbCl_3 \cdot 6H_2O$ (99.99%), $ErCl_3 \cdot 6H_2O$ (99.9%), NaOH (98%), NH_4F (98%), 1-octadecene (90%), oleic acid (90%), poly(acrylic acid) (PAA), poly(allylamine hydrochloride) (PAH), lysozyme, thrombin and bovine serum albumin (BSA) were purchased from Sigma-Aldrich. All oligonucleotides were supplied by Sangon Biotechnology Co., Ltd (Shanghai, China). Serum mixture specimens of one hundred healthy persons were provided by the Affiliated Drum Tower Hospital of Nanjing University. Other chemical reagents of analytical grade were used directly without further purification. Ultrapure water (Milli-Q, Millipore) was used throughout. The sequences of oligonucleotides used in this work are as follows:

Lysozyme aptamer: 5′-ATC AGG GCT AAA GAG TGC AGA GTT ACT TAG-TAMRA-3′

Target DNA: 5′-CTA AGT AAC TCT GCA CTC TTT AGC CCT GAT-3′

2.2 Synthesis of OA-UCNPs

The synthesis of $NaYF_4$: 18% Yb, 2% Er nanoparticles was developed *via* a modified literature procedure.[33] In a typical experiment, 1 mmol $RECl_3$ (0.80 mmol YCl_3, 0.18 mmol $YbCl_3$ and 0.02 mmol $ErCl_3$) was added into a 100 mL flask containing 7.5 mL oleic acid and 15 mL 1-octadecene. The solution was heated to 160 °C under a nitrogen atmosphere for 30 min and then cooled down to room temperature. Thereafter, 10 mL methanol solutions containing NH_4F (4.0 mmol) and NaOH (2.5 mmol) were added into the solution and stirred for 30 min. After the methanol evaporated, the solution was heated to 300 °C under a nitrogen atmosphere for 1 h and cooled down to room temperature. The resulting nanoparticles were precipitated by the addition of ethanol, collected by centrifugation, washed with ethanol and water several times, and finally redispersed in toluene.

2.3 Transferring hydrophobic OA-UCNPs to hydrophilic PAA-UCNPs through ligand exchange

The strategy was developed *via* a modified literature procedure.[34] Typically, 0.60 g of PAA was added to 12 mL diethylene glycol (DEG) and the mixture was heated to 110 °C with vigorous stirring under a nitrogen atmosphere. A toluene solution of the OA-UCNPs (30 mg of OA-UCNPs in 2 mL toluene) was added to the system and then heated to 240 °C and kept at the temperature for 1 h. After the solution was cooled down to room temperature, excess dilute hydrochloric acid aqueous solution (0.1 M) was added, and a white powder was obtained by centrifuging. The powder was washed three times with pure water and could be well dispersed into water and buffer solution.

2.4 Loading PAH onto PAA-UCNPs for assembly of PAH–PAA-UCNPs (ppUCNPs)

10 mg of the as-prepared PAA-UCNPs was redissolved in water (pH 8.5) and 10 mg mL^{-1} PAH solution (containing 20 mM NaCl) was added to the system. The mixture was stirred for 1 h at room temperature and the solid was collected by centrifuging (16 000 rpm, 10 min), then the collected solid was repeatedly washed with water to remove the unbounded polymer. The obtained positively charged PAH–PAA-UCNPs (ppUCNPs) were dispersed into Tris–HCl buffer (20 mM, containing 10 mM NaCl and 10 mM $MgCl_2$, pH 7.4) and used for subsequent experiments.

2.5 Attachment of the aptamer to ppUCNPs

The obtained ppUCNPs were modified by the aptamer labeled with 6-carboxytetramethylrhodamine (TAMRA) at the 3′ end (TAMRA-aptamer). 2 mg ppUCNPs were diluted with 2 mL Tris–HCl buffer (20 mM, containing 10 mM NaCl and 10 mM $MgCl_2$, pH 7.4) and incubated with TAMRA-aptamer (1 μM) at 30 °C for 30 min. The ppUCNPs attached with the aptamer (ppUCNPs-aptamer) were harvested with centrifugation and washing. Finally, the product was diluted with 2 mL Tris–HCl buffer (20 mM, containing 10 mM NaCl and 10 mM $MgCl_2$, pH 7.4) and stored at 4 °C for further use.

2.6 Upconversion fluorescence experiments

In a typical UCNPs-based FRET assay procedure, the ppUCNPs-aptamer (200 μL) and various concentrations of lysozyme or the target DNA were mixed in tubes. After adjusting the total volume to 600 μL with the buffer, the system was incubated at 30 °C for 80 min. The upconversion luminescence (UCL) spectra of the final mixture were recorded on a ZolixScan ZLX-UPL spectrometer with an external 980 nm laser as the excitation source. To assess the specificity of the sensor, four other biomolecules including α-amylase, bovine serum albumin (BSA), thrombin and glycine (Gly) were added to the system following an identical procedure. To verify the ability of the method to resist background interference, lysozyme detection was performed in human saliva and serum samples.

Human saliva samples were collected from 3 healthy volunteers in the morning before breakfast. The samples were recollected without the precipitate. 40 μL of the saliva sample solution and 200 μL of the ppUCNPs-aptamers were mixed in tubes, and the total volume was adjusted to 600 μL with the buffer. The recovery experiment was carried out by adding 30 nM of standard lysozyme solution to the system. After 80 min of incubation at 30 °C, the system was taken for the UCL measurement. Human serum mixture samples were collected from 100 healthy adults in the Affiliated Drum Tower Hospital of Nanjing University according to their standard clinical procedures. The determination process was similar to that of saliva except that 100 μL of the serum samples instead of saliva samples were used.

2.7 Characterization

The morphology and structure were characterized by transmission electron microscopy (TEM) using a JEOL-2100 TEM operating at 200 kV. Energy-dispersive X-ray (EDX) analysis spectra were obtained by a field-emission scanning electron microscope (Hitachi S4800, Japan) equipped with an EDAX Genesis analysis system. X-ray powder diffraction (XRD) measurements were performed on a Japan Shimadzu XRD-6000 diffractometer with Cu-Kα radiation ($\lambda = 0.15418$ nm), and a scanning rate of 0.05 deg s^{-1} was applied to record the patterns in the 2θ range of 10–80°. Zeta potential was measured on a Nano-Z Zetasizer. The UV-vis absorption and the Fourier transform infrared (FT-IR) spectra were obtained using a UV-3600 spectrophotometer and a NICOLET iS10 FT-IR spectrometer, respectively. Upconversion fluorescence spectra were recorded on a ZolixScan ZLX-UPL spectrometer using an external 1 W continuous-wave laser (980 nm) as the excitation source.

3. Results and discussion

3.1 Principle of the FRET aptasensor for lysozyme detection

A new platform for lysozyme and the target DNA detection was developed with positive upconversion nanoparticles (ppUCNPs) and a dye labeled aptamer as the FRET pair. As shown in Scheme 1, oleic acid capped UCNPs (OA-UCNPs) were first synthesized using a hydrothermal route, and the as-prepared materials could be well dispersed into nonpolar organic solvents (toluene, hexane, chloroform *etc.*) to form stable colloids due to the presence of the hydrophobic oleate anion. Bio-applications are usually carried out in aqueous solution, therefore proper dispersion of the nanoparticles in water was required. To this end, two surface modification steps were performed on the as-prepared OA-UCNPs. PAA which served as a multidentate ligand was first chosen to exchange the original hydrophobic ligands on the surface of UCNPs. To attach the negatively charged DNA, an additional layer of PAH was coated onto the PAA-UCNPs surface, and positively charged ppUCNPs were obtained. The sensor was set up by coating the dye labeled aptamer on the surface of the ppUCNPs, and TAMRA was

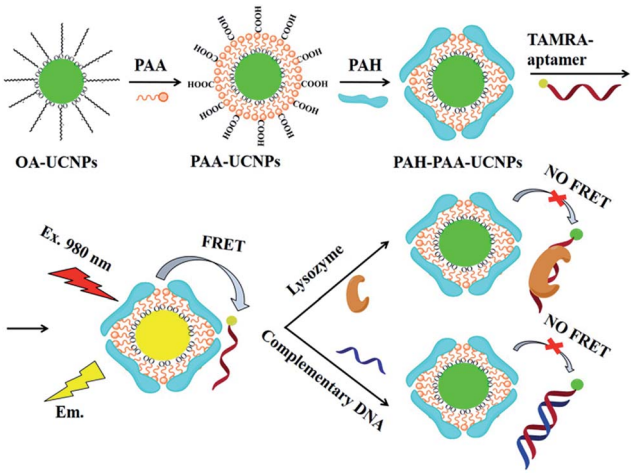

Scheme 1 Schematic illustration of the FRET biosensor for lysozyme and DNA detection based on UCNPs.

selected as the dye molecule labeled on the aptamer (abbreviated as TAMRA-aptamer).

In Fig. 1, we can observe that the UV-vis absorption spectrum of TAMRA-aptamer (acceptor) overlaps well with the fluorescence emission band centered at 520 and 543 nm of the UCNPs (donors), which can be attributed to the $^2H_{11/2} \rightarrow {}^4I_{15/2}$ and $^4S_{3/2} \rightarrow {}^4I_{15/2}$ transitions of Er^{3+}, respectively. Meanwhile, red emission at around 655 nm, assigned to the $^4F_{9/2} \rightarrow {}^4I_{15/2}$ transition of Er^{3+},[35] should remain without change since it is far away from the absorption band of TAMRA. To avoid possible interference, UCL at 655 nm can be taken as a reference to the green emission to allow ratiometric detection. With static electricity interaction, TAMRA-aptamer can be brought in close proximity to the ppUCNPs and the FRET from UCNPs to TAMRA occurs under the excitation at 980 nm. Upon the addition of lysozyme to the system, the TAMRA-aptamer was far away from the ppUCNPs due to the high affinity and specificity between

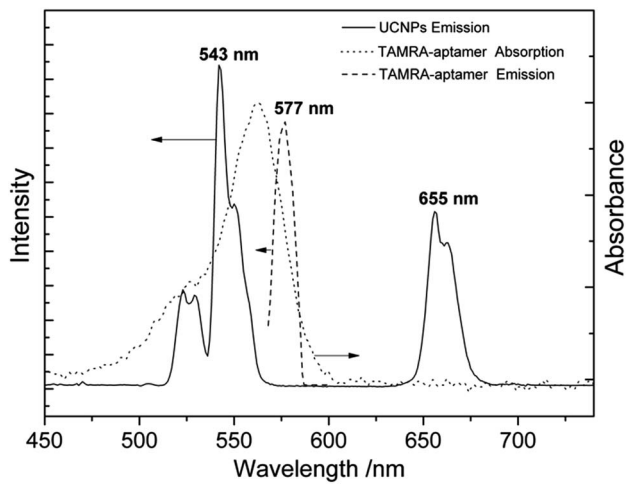

Fig. 1 The absorption (dot line) and emission (short dash line) spectra of TAMRA-aptamer aqueous solution besides the emission spectrum (solid line) of the UCNPs.

the aptamer and lysozyme. As a result, the luminescence of the ppUPCNs was restored. Similarly, when the target DNA was introduced into the system, a DNA duplex structure (dsDNA) forms due to the hybridization between the aptamer and the target DNA. As a result, the distance between the ppUCNPs and TAMRA-aptamer increased and the UCL was restored. The results showed that the relative UCL intensity was related to the concentration of lysozyme or the target DNA.

3.2 Characterization of the materials

$NaYF_4$:Yb,Er was selected as the upconversion donor since it has so far been the most efficient NIR-to-visible upconversion material due to the low phonon energy of $NaYF_4$ as the host matrix.[5] Extremely strong green emission was obtained and only a slight fluorescence change could be observed after PAA and PAH modification (Fig. S1†), so it has no influence on luminescence measurement. Fig. 2 presents representative TEM images of the as-prepared and modified upconversion particles. The monodisperse nanospheres of the as-prepared samples have an average size of about 29.0 nm (Fig. 2A and D) and the size changed little after the two step modification (Fig. 2B and C). The TEM images also indicated that the as-prepared nanoparticles (OA-UCNPs) were well dispersed into nonpolar solvents (cyclohexane, chloroform for example) and the modified ones (PAA-UCNPs and ppUCNPs) could be easily dispersed into water. EDX analysis confirmed the presence of Na, F, Y, Yb and Er in the three samples and no obvious changes in the composition of $NaYF_4$, Yb, Er were observed (Fig. S2†). XRD patterns of OA-UCNPs and PAA-UCNPs reveal that both samples have similar phases, which can be indexed to the pure hexagonal phase of $NaYF_4$ (JCPDS no. 28-1192) (Fig. 3A).

The capping ligands on the surface of the nanoparticles were identified by FT-IR spectra (Fig. 3B). All the three samples exhibit a broad band around 3450 cm^{-1} which corresponds to the O–H stretching vibration. The peaks at 2924 and 2856 cm^{-1} are assigned to the asymmetric (ν_{as}) and symmetric (ν_s) stretching vibrations of methylene (–CH_2–) in the long alkyl chain of oleic acid; these two peaks become unconspicuous after the modification. The peak at 3003 cm^{-1} attributed to the group =CH_2 can be clearly seen in the spectrum of OA-UCNPs,[36] while it disappears after the modification. In addition, the peaks at 1558 and 1462 cm^{-1} can be assigned to the asymmetric (ν_{as}) and symmetric (ν_s) stretching vibrations of the carboxylic group in oleic acid. After ligand exchange by PAA, the two peaks shift a little and two new peaks at 1732 and 1396 cm^{-1} related to the carboxylic group appear, indicating that the primary ligand oleic acid was successfully exchanged by PAA. Upon the attachment of PAH, the peak at 1732 decreased and a weak peak at 740 cm^{-1} resulting from the bending vibration of the N–H bond in PAH could be found,[17] which confirmed that ppUCNPs were formed finally. The process was also verified by zeta potential spectroscopy. The zeta potential of the nanocomposites changed from negative (−37.8 mV) to positive (+37.4 mV) alternated after PAA and PAH modification, while the potential was found to be −9.19 mV after the addition of TAMRA-aptamer (1 μM). The zeta results further indicated that the process was realized as expected.

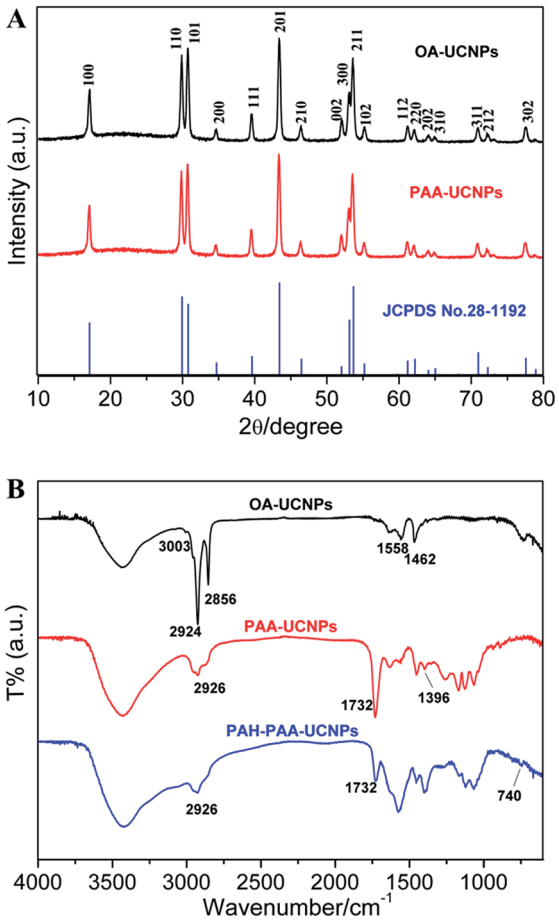

Fig. 3 XRD pattern (A) and FT-IR spectra (B) of the as-prepared and modified UCNPs.

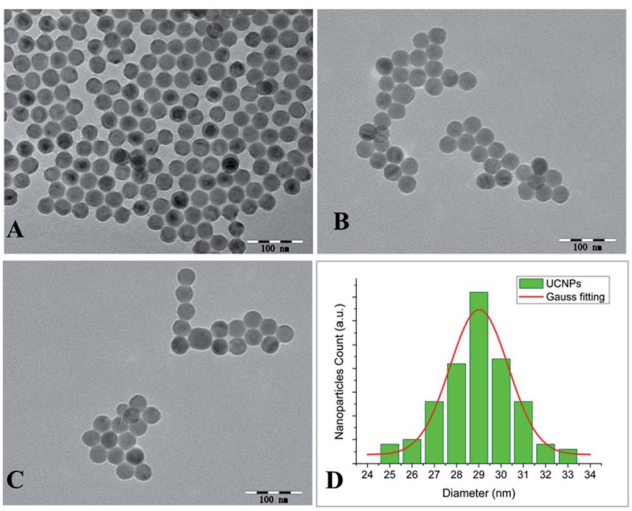

Fig. 2 TEM images of OA-UCNPs (A, in cyclohexane), PAA-UCNPs (B, in water), ppUCNPs (C, in water), and the histogram of particle size for OA-UCNPs, data were obtained from the TEM images of more than 300 upconversion particles with R-squared value 0.94 (D).

3.3 FRET between ppUCNPs and TAMRA induced through the aptamer

In order to attach more TAMRA-aptamer and obtain high FRET efficiency, the excess of the unbounded cationic polymer PAH in the positive UCNPs solution had to be minimized. An experiment was carried out by gradually adding PAH to a solution containing PAA-UCNPs, and zeta potential was measured (Fig. 4A), the results showed that the zeta potential reached its maximum at the concentration of 0.75 mg mL^{-1}. As shown in Fig. 4B, when lysozyme was added to the ppUCNPs-aptamer solution, the UCL intensity increased slowly within 80 min incubation. After that, the intensity was virtually unchanged. So

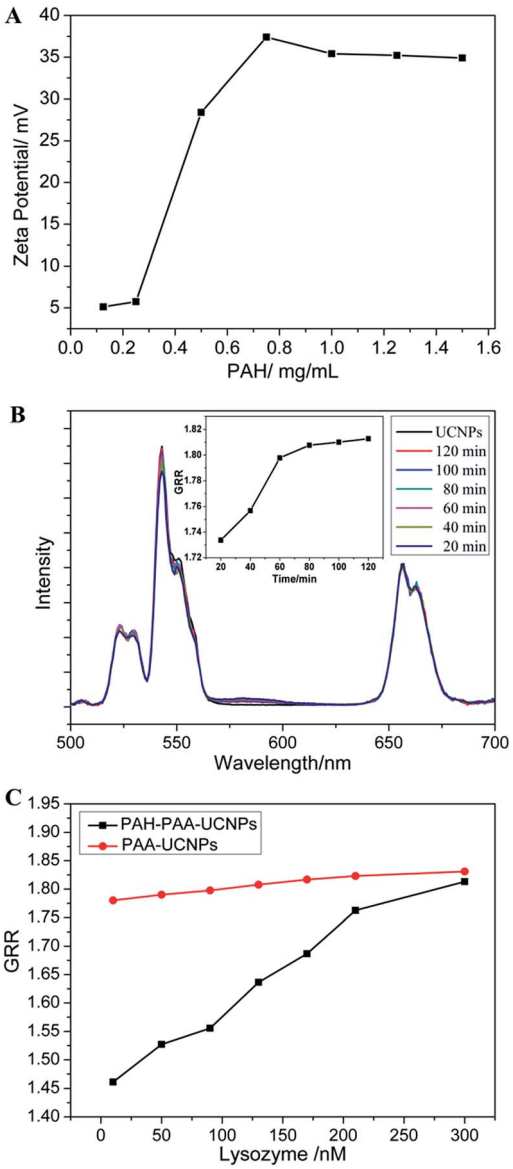

Fig. 4 Zeta potential changes with the addition of PAH (A). Time dependence of the fluorescence recovery of the ppUCNPs-aptamer complex upon the addition of 300 nM lysozyme; inset: the green to red ratio (GRR, $UCL_{510-565}/UCL_{640-680}$) of UCL intensity at different times (B). The green to red ratio of UCL intensity with different lysozyme concentrations before and after PAH modification (C).

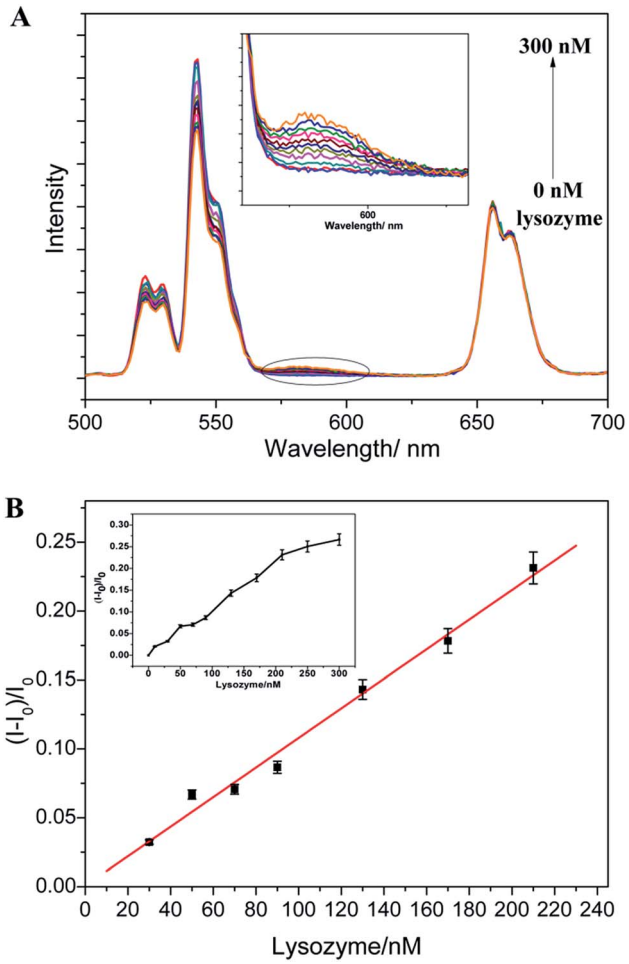

Fig. 5 UCL spectra of the sensor with various concentrations of lysozyme, inset: amplified UCL spectra around 580 nm (A). The linear relationship of the relative fluorescence intensity *versus* the concentration of lysozyme in the range from 30 to 210 nM; inset: fluorescence recovery of the sensor in the presence of 0–300 nM lysozyme. I_0 and I denote the relative fluorescence intensity $UCL_{510-565}/UCL_{640-680}$ before and after addition of lysozyme (B).

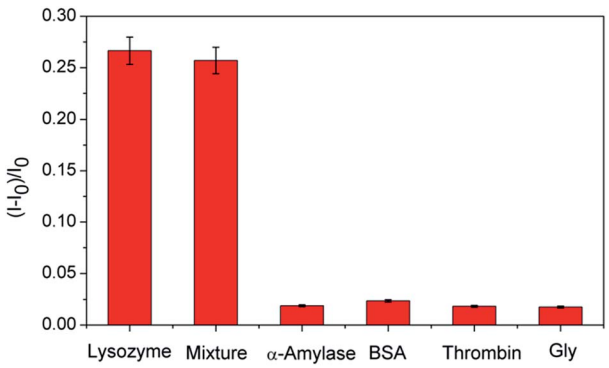

Fig. 6 Specificity of the aptamer-ppUCNPs toward other molecules. Mixture represents the mixture of lysozyme and the other four molecules. The concentration of α-amylase and Gly was 15.0 mg L^{-1} and 3 mM respectively, the concentration of the other three molecules was 300 nM.

Table 1 Lysozyme recovery in diluted human saliva ($n = 4$)

Sample	Measured (nM)	Added (nM)	Found (nM)	Recovery (%)	RSD (%)
1	95.3	30	114.2	91.1	3.3
2	143.1	30	179.1	103.5	2.1
3	121.0	30	143.7	95.2	2.6

0.75 mg mL^{-1} PAH was needed and the UCL measurement was carried out after incubating for 80 min. To confirm the adsorption of PAH, a control experiment was conducted where PAA-UCNPs (without PAH modification) at 0.2 mg mL^{-1} with different concentrations of lysozyme were incubated with TAMRA-aptamer (1 μM). In this case, the UCL intensity was restored a little and the green to red ratio (GRR, $UCL_{510–565}$/$UCL_{640–680}$, $UCL_{A–B}$ are the integrated emission intensities from A to B nm) changed slightly compared with that using ppUCNPs (Fig. 4C).

3.4 Analysis of lysozyme and the target DNA

The UCL of the UPCNs was quenched with the addition of TAMRA-aptamer (1 μM). When increasing amounts of lysozyme were introduced into the system, the emission intensity of the UCNPs was restored gradually. This can be explained by the separation of the acceptor from the donor because the TAMRA-aptamer prefers combining with lysozyme to ppUCNPs. The relative fluorescence intensity was linearly related to the concentration of lysozyme ranging from 30 to 210 nM (Fig. 5) and the limit of detection (LOD) of lysozyme is as low as 2.8 nM calculated by 3SD/m, where 3 is the factor at the 99% confidence level, SD represents the standard deviation of the blank measurements ($n = 8$) and m is the slope for the range of linearity.[15,37] The sensor can also be used in DNA determination, and the relative fluorescence intensity was also linearly related to the concentration of the target DNA in the range of 40 to 200 nM with the LOD of 2.8 nM (Fig. S3†).

3.5 Specificity evaluation and analytical application

To examine the specificity of the sensor for lysozyme, control experiments were performed with the fixed concentration of aptamer-ppUCNPs in the presence of α-amylase, BSA, thrombin and Gly, respectively. In addition, a mixture of lysozyme and the four non-specific biomolecules was also tested. As shown in Fig. 6, obvious response was observed when lysozyme or the mixture of lysozyme and the four non-specific biomolecules was added to the assay system, whereas the non-specific biomolecules gave little response. The results show the high selectivity of this method.

The method was applied to detect lysozyme levels in human saliva samples. Taking the dilution into account in the calculation, the obtained values are between 1.4 and 2.1 μM (Table S1†), which are consistent with the normal range of the reported literature.[31,38] To further validate the developed method, 30 nM of lysozyme was added to the diluted saliva samples. The recoveries were in the range from 91.1% to 103.5% with a relative standard deviation (RSD) around 3% (Table 1), indicating a high level of accuracy of the developed assay. To broaden the application, the concentrations of lysozyme in human serum were also measured, and the results shown in Table S2† were within the normal range of the reported literature.[39,40] The results indicate that the developed sensor is applicable in such a complicated matrix, which shows its potential use in biological and clinical applications.

4. Conclusions

In summary, we have fabricated a novel upconversion FRET sensing platform for the determination of lysozyme as well as DNA. The energy transfer occurs between the upconversion nanoparticles and the dye labeled aptamer, and a cationic polymer that acted as an electrostatic linker was used to bring the donor and acceptor into close proximity. However, in the presence of lysozyme or the complementary DNA, fluorescence recovery was observed, and the relative recovery intensity was proportional to its concentration. The method shows high sensitivity as well as good selectivity, and because it is a label-free method without covalent linking, the assay is fairly simple and convenient. Besides, UCNPs as excellent emitters with their low autofluorescence and high penetration depth endow this system with further potential applications in biological and analytical fields. Therefore, we believe that this general method can be extended to numerous other fluorescent sensing probes and may be put into practice in determining lysozyme in human samples.

Acknowledgements

We greatly appreciate the financial support from the National Natural Science Foundation of China (NSFC) (no. 21171091, 21335004, 21405001) and the support from 973 Program (no. 2011CB933502). The authors extend their appreciation to the State Key Laboratory of Analytical Chemistry for Life science (SKLACLS1307).

Notes and references

1 L. D. Sun, Y. F. Wang and C. H. Yan, *Acc. Chem. Res.*, 2014, **47**, 1001.
2 Y. S. Liu, S. Y. Zhou, D. T. Tu, Z. Chen, M. D. Huang, H. M. Zhu, E. Ma and X. Y. Chen, *J. Am. Chem. Soc.*, 2012, **134**, 15083.
3 F. Wang and X. G. Liu, *Chem. Soc. Rev.*, 2009, **38**, 976.

4 S. J. Wu, N. Duan, Z. P. Wang and H. X. Wang, *Analyst*, 2011, **136**, 2306.
5 S. Gai, C. X. Li, P. P. Yang and J. Lin, *Chem. Rev.*, 2014, **114**, 2343.
6 Y. J. Ding, X. Teng, H. Zhu, L. L. Wang, W. B. Pei, J. J. Zhu, L. Huang and W. Huang, *Nanoscale*, 2013, **5**, 11928.
7 J. Zhou, Z. Liu and F. Y. Li, *Chem. Soc. Rev.*, 2012, **41**, 1323.
8 D. J. Naczynski, M. C. Tan, R. E. Riman and P. V. Moghe, *J. Mater. Chem. B*, 2014, **2**, 2958.
9 J. W. Liu, Z. H. Cao and Y. Lu, *Chem. Rev.*, 2009, **109**, 1948.
10 J. C. Cox and A. D. Ellington, *Bioorg. Med. Chem.*, 2001, **9**, 2525.
11 X. H. Fang and W. H. Tan, *Acc. Chem. Res.*, 2010, **43**, 48.
12 Y. H. Wang, P. Shen, C. Y. Li, Y. Y. Wang and Z. H. Liu, *Anal. Chem.*, 2012, **84**, 1466.
13 M. Schifferer and O. Griesbeck, *J. Am. Chem. Soc.*, 2012, **134**, 15185.
14 H. Kim, C. Y. W. Ng and W. R. Algar, *Langmuir*, 2014, **30**, 5676.
15 K. Song, X. G. Kong, X. M. Liu, Y. L. Zhang, Q. H. Zeng, L. P. Tu, Z. Shi and H. Zhang, *Chem. Commun.*, 2012, **48**, 1156.
16 J. L. Liu, J. T. Cheng and Y. Zhang, *Biosens. Bioelectron.*, 2013, **43**, 252.
17 L. Y. Wang, R. X. Yan, Z. Y. Hao, L. Wang, J. H. Zeng, H. Bao, X. Wang, Q. Peng and Y. D. Li, *Angew. Chem., Int. Ed.*, 2005, **44**, 6054.
18 Y. Cen, Y. M. Wu, X. J. Kong, S. Wu, R. Q. Yu and X. Chu, *Anal. Chem.*, 2014, **86**, 7119.
19 Z. G. Chen, H. L. Chen, H. Hu, M. X. Yu, F. Y. Li, Q. Zhang, Z. G. Zhou, T. Yi and C. H. Huang, *J. Am. Chem. Soc.*, 2008, **130**, 3023.
20 Y. J. Ding, H. Zhu, X. X. Zhang, J. J. Zhu and C. Burda, *Chem. Commun.*, 2013, **49**, 7797.
21 S. J. Wu, N. Duan, X. Y. Ma, Y. Xia, H. Wang, Z. P. Wang and Q. Zhang, *Anal. Chem.*, 2012, **84**, 6263.
22 C. H. Liu, Z. Wang, H. X. Jia and Z. P. Li, *Chem. Commun.*, 2011, **47**, 4661.
23 L. Y. Zeng, Y. X. Yuan, P. Shen, K. Y. Wong and Z. H. Liu, *Chem.–Eur. J.*, 2013, **19**, 8063.
24 Y. H. Wang, Z. J. Wu and Z. H. Liu, *Anal. Chem.*, 2013, **85**, 258.
25 L. L. Li, P. W. Wu, K. Hwang and Y. Lu, *J. Am. Chem. Soc.*, 2013, **135**, 2411.
26 S. Y. Liu, W. D. Na, S. Pang, F. P. Shi and X. G. Su, *Analyst*, 2014, **139**, 3048.
27 S. S. Levinson, R. J. Elin and L. Yam, *Clin. Chem.*, 2002, **48**, 1131.
28 S. Bamrungsap, M. I. Shukoor, T. Chen, K. Sefah and W. H. Tan, *Anal. Chem.*, 2011, **83**, 7795.
29 B. Wang and C. Yu, *Angew. Chem., Int. Ed.*, 2010, **49**, 1485.
30 J. Huang, Z. Zhu, S. Bamrungsap, G. Z. Zhu, M. X. You, X. X. He, K. M. Wang and W. H. Tan, *Anal. Chem.*, 2010, **82**, 10158.
31 D. Tang, D. L. Liao, Q. K. Zhu, F. Y. Wang, H. P. Jiao, Y. J. Zhang and C. Yu, *Chem. Commun.*, 2011, **47**, 5485.
32 Y. Y. Wang, K. Y. Pu and B. Liu, *Langmuir*, 2010, **26**, 10025.
33 Z. Q. Li, Y. Zhang and S. Jiang, *Adv. Mater.*, 2008, **20**, 4765.
34 C. H. Liu, H. Wang, X. Li and D. P. Chen, *J. Mater. Chem.*, 2009, **19**, 3546.
35 Y. H. Zhang, L. X. Zhang, R. R. Deng, J. Tian, Y. Zong, D. Y. Jin and X. G. Liu, *J. Am. Chem. Soc.*, 2014, **136**, 4893.
36 L. Y. Wang and Y. D. Li, *Nano Lett.*, 2006, **6**, 1645.
37 L. Shang, H. J. Chen, L. Deng and S. J. Dong, *Biosens. Bioelectron.*, 2008, **23**, 1180.
38 C. Tsang and L. Samaranayake, *Oral Dis.*, 1999, **5**, 241.
39 J. Hankiewicz and E. Swierczek, *Clin. Chim. Acta*, 1974, **57**, 205.
40 T. Jing, H. R. Du, Q. Dai, H. Xia, J. W. Niu, Q. L. Hao, S. R. Mei and Y. K. Zhou, *Biosens. Bioelectron.*, 2010, **26**, 301.

